Natural variation in meiotic recombination rate shapes introgression patterns in intraspecific hybrids between wild and domesticated barley

Steven Dreissig[1] (iD), Andreas Maurer[1] (iD), Rajiv Sharma[2], Linda Milne[3], Andrew John Flavell[2], Thomas Schmutzer[1] (iD) and Klaus Pillen[1] (iD)

[1]Institute of Agricultural and Nutritional Sciences, Martin Luther University Halle-Wittenberg, Betty-Heimann-Straße 3, Halle (Saale) 06120, Germany; [2]Division of Plant Sciences, University of Dundee at JHI, Invergowrie, Dundee, DD2 5DA, UK; [3]The James Hutton Institute (JHI), Invergowrie, Dundee, DD2 5DA, UK

Authors for correspondence:
Steven Dreissig
Tel: +49 345 55 22 683
Email: steven.dreissig@landw.uni-halle.de

Klaus Pillen
Tel: +49 345 55 22 680
Email: klaus.pillen@landw.uni-halle.de

Summary

- Meiotic recombination rates vary considerably between species, populations and individuals. The genetic exchange between homologous chromosomes plays a major role in evolution by breaking linkage between advantageous and deleterious alleles in the case of introgressions. Identifying recombination rate modifiers is thus of both fundamental and practical interest to understand and utilize variation in meiotic recombination rates.
- We investigated recombination rate variation in a large intraspecific hybrid population (named HEB-25) derived from a cross between domesticated barley and 25 wild barley accessions.
- We observed quantitative variation in total crossover number with a maximum of a 1.4-fold difference between subpopulations and increased recombination rates across pericentromeric regions. The meiosis-specific α-kleisin cohesin subunit *REC8* was identified as a candidate gene influencing crossover number and patterning. Furthermore, we quantified wild barley introgression patterns and revealed how local and genome-wide recombination rate variation shapes patterns of introgression.
- The identification of allelic variation in *REC8* in combination with the observed changes in crossover patterning suggest a difference in how chromatin loops are tethered to the chromosome axis, resulting in reduced crossover suppression across pericentromeric regions. Local and genome-wide recombination rate variation is shaping patterns of introgressions and thereby directly influences the consequences of linkage drag.

Introduction

Introgression is the transfer of genetic material between or within species through hybridization followed by backcrossing. Both interspecific and intraspecific introgressions are widespread in nature, as revealed by recent genome-scale sequence data (Mallet *et al.*, 2016). As such, adaptive introgressions have been found in plants, humans, butterflies and birds (Heliconius Genome Consortium, 2012; Huerta-Sánchez *et al.*, 2014; Lamichhaney *et al.*, 2015; Arnold *et al.*, 2016). Hybridization between wild and domesticated species is commonly used in plant breeding to develop new cultivars possessing desirable traits (Hufford *et al.*, 2012; Wendler *et al.*, 2014; Maurer *et al.*, 2015; He *et al.*, 2019). The genomic landscape of introgressions is influenced by selection, drift and recombination (Martin & Jiggins, 2017). Introgressions may simultaneously introduce beneficial and deleterious alleles. In these cases, the efficacy of selection depends partially on the local recombination rate in order to break linkage between beneficial and deleterious alleles. Linkage drag is of hindrance in plant breeding, where deleterious alleles are introgressed along with a desired beneficial allele (Young & Tanksley, 1989). Therefore, both local and genome-wide recombination rate variation play an important role in shaping the evolution of naturally occurring hybrid genomes and the genetic gain achieved in plant breeding (Schumer *et al.*, 2018; Tourrette *et al.*, 2019).

Meiotic recombination and the random segregation of chromosomes are fundamental features of eukaryotic sexual reproduction and give rise to novel allelic combinations. Recombination takes place during meiotic prophase and is initiated by a programmed formation of DNA double-strand breaks (DSBs) via SPO11 complexes (Lam & Keeney, 2014). Meiotic DSBs are processed by protein complexes to be repaired via synthesis-dependent strand annealing (SDSA) or homologous recombination (HR), which may result in crossovers or noncrossovers (Mercier *et al.*, 2015). Meiotic recombination takes place when

chromosomes are associated with a proteinaceous structure, the synaptonemal complex, which mediates DSB repair, chromosome pairing and segregation (Zickler & Kleckner, 1999; Page & Hawley, 2003; Börner *et al.*, 2004). As such, meiotic recombination rates depend on chromatin context, are affected by crossover interference (i.e. physical interference between neighbouring crossovers along the chromosome), crossover assurance (i.e. one obligatory crossover per chromosome to ensure correct pairing and segregation), crossover homeostasis (i.e. maintenance of a stable crossover number under varying levels of initial DSBs), and are shaped by the spatiotemporal order of meiosis (Higgins *et al.*, 2012; Zhang *et al.*, 2014; Yelina *et al.*, 2015; Zelkowski *et al.*, 2019). Furthermore, the position of the centromere and nucleolus organizer regions (NORs) were shown to locally suppress meiotic crossovers (Fernandes *et al.*, 2019; Sims *et al.*, 2019). Although this process is essentially conserved across eukaryotes, genome-wide recombination rates (GWRRs) are surprisingly variable between species, populations, sexes and individuals (Wang *et al.*, 2012; Stapley *et al.*, 2017; Haenel *et al.*, 2018; Kianian *et al.*, 2018). At the chromosome scale, recombination rates tend to be drastically reduced near centromeric regions (Künzel *et al.*, 2000; Choi *et al.*, 2013; Darrier *et al.*, 2017; Dreissig *et al.*, 2019). This reduction across pericentromeric regions is influenced by epigenetic information, such as DNA methylation, histone modifications and nucleosome positions (Mirouze *et al.*, 2012; Melamed-Bessudo & Levy, 2012; Yelina *et al.*, 2012; Choi *et al.*, 2013, 2018; Underwood *et al.*, 2018). Additionally, genetic divergence and structural variations are also influencing recombination rates (Ziolkowski *et al.*, 2015, 2017; Crown *et al.*, 2018; Rowan *et al.*, 2019). At the population level, recombination rates were shown to vary drastically depending on variations in meiotic genes or environmental conditions (Brand *et al.*, 2018; Dreissig *et al.*, 2019; Martin *et al.*, 2019; Samuk *et al.*, 2019; Schwarzkopf *et al.*, 2020).

In the present study, we explore the association of genotypes with variation in recombination rates of the nested-association mapping population HEB-25 (Maurer *et al.*, 2015), which consists of 25 intraspecific subpopulations derived from hybridization between domesticated and wild barley (*Hordeum vulgare* (cv. Barke) × *Hordeum vulgare* subsp. *spontaneum*). We investigate how recombination rate variation directly affects genomic patterns of introgression. By comparing genome-wide recombination landscapes among the 25 subpopulations, we observe quantitative variation in the total number of crossovers as well as crossover patterning, with an increase across pericentromeric regions in high- vs low-recombining subpopulations. We identify the meiosis-specific α-kleising cohesin subunit REC8 as a putative genome-wide recombination rate modifier. Utilizing genome-wide recombination rate variation among the 25 subpopulations, we provide empirical evidence regarding how the size and distribution of introgressions is shaped by recombination. Together, our study links variation in recombination rate to allelic variation in a meiotic gene involved in tethering chromatin loops to the chromosome axis and provides experimental evidence for the relationship between recombination rate variation and patterns of introgression.

Materials and Methods

Plant material and SNP array genotyping

In this study, we used a large intraspecific hybrid population (HEB-25) derived from a cross between the domesticated barley cultivar 'Barke' (*Hordeum vulgare* L.) and 25 wild barley (*Hordeum vulgare* subsp. *spontaneum* (K. Koch) Thell) accessions previously developed by Maurer *et al.* (2015). This population is composed of 25 subpopulations with between 21 and 72 $BC_1S_{3:8}$ lines per subpopulation (i.e. one backcross to the domesticated barley parent and eight generations of selfing), resulting in a total of 1340 lines. Plants were grown under field conditions from 2011 until 2018 in central Germany (Halle (Saale), 51°29′45.6″ N, 11°59′40.2″E). DNA of 12 pooled individual plants of each $BC_1S_{3:8}$ line was extracted using the Qiagen BioSprint 96 DNA Plant Kit and a BioSprint workstation following the manufacturer's instructions. Single nucleotide polymorphism (SNP) genotyping was performed by TraitGenetics (Gatersleben, Germany) for all 1340 lines on the barley 50k iSelect SNP array (Bayer *et al.*, 2017). SNP markers that did not meet the quality criteria (polymorphic in at least one HEB family, < 10% failure rate, < 12.5% heterozygous calls) were removed from the dataset. Furthermore, 256 redundant SNPs were removed as they showed the exact same segregation among all HEB lines, indicating that they were in complete linkage disequilibrium (LD). Only one of these markers was kept. SNP raw data were deposited on e!DAL under the following https://doi.org/10.5447/ipk/2019/20 (Arend *et al.*, 2014; Maurer & Pillen, 2019). Physical map positions of all SNPs according to the most recent reference sequence of the barley genome (TRITEX Morex V2) (Monat *et al.*, 2019) were downloaded from https://ics.hutton.ac.uk/50k/.

Crossover counting, recombination landscape and introgression analysis

All the following analyses were done using basic functions of the R statistical environment if not stated otherwise (R Core Team, https://www.rproject.org/contributors.html). To count crossovers, the entire SNP matrix containing raw data was first converted into numerical format, where the 'Barke' allele is coded as 0, heterozygous alleles are coded as 1 and wild barley alleles are coded as 2. The entire SNP matrix was then split into subpopulation matrices from which subpopulation-specific monomorphic markers were removed, as well as markers with missing values. Subpopulation SNP matrices were further filtered against a minor allele frequency of <0.1. Finally, to avoid false positive crossover counts caused by small structural variations or falsely assigned physical positions, we aggregated SNPs by counting the most common allele in sliding windows of a size of 20 consecutive SNPs using the SlidingWindow() function of the EVOBIR package (Blackmon *et al.*, 2015) of the R statistical environment. Thereby, single markers giving rise to suspicious double crossovers were removed. Using the aggregated SNP matrix of each subpopulation, crossovers were then counted as changes in the allelic state along the physical length of the chromosome. The

total crossover count (TCO) of each line was used to calculate the mean crossover number per subpopulation, and lines showing more than 60 crossovers (37 out of 1340 lines) were removed as outliers. Outliers were removed based on strong deviations from the population mean, that is outside the three-fold interquartile range. The 37 outliers showed a mean TCO of 103.19 compared to a population mean of 24.38, and an outlier-pruned population mean of 22.17 (Supporting Information Fig. S2). ANOVA was performed to test for differences among the entire population and Tukey's honest significant difference (HSD) test was performed to test for multiple pairwise differences between subpopulations. Crossover data are summarized in Dataset S1. To analyse the recombination landscape of each subpopulation, we summarized recombination frequencies between pairs of SNPs in 1 Mb intervals multiplied by a factor of 100 to obtain cM Mb^{-1} values along the physical length of the chromosome. Our ability to detect recombination events decreased with each generation due to a decrease in heterozygosity of 50% per generation caused by self-pollination. Using this approach, we systematically underestimated the true per-generation recombination rate, because individuals of our HEB-25 population were genotyped after nine rounds of meiosis. Mitotic recombination events in the tissue which gave rise to meiocytes could potentially have contributed to the total number of crossovers detected as well. Therefore, recombination rates reported here should not be interpreted as a per-generation recombination rate. Recombination landscapes of each chromosome of each subpopulation were visualized by plotting recombination rates in 1 Mb intervals (cM Mb^{-1}) against their physical position. To compare the genome-wide recombination landscapes of selected subpopulations, we calculated the mean recombination rate across all seven chromosomes in relative chromosomal intervals of 0.5%, where the physical length of each chromosome was normalized to range from 0 to 100%. We then split the relative length of the chromosome into three intervals (e.g. 0–25%, 25–75%, 75–100%) and used cM Mb^{-1} values in 0.5% intervals to perform Welch's two-sample t-tests to infer significant differences between subpopulations. The same approach was used to compare SNP densities between subpopulations, for which SNPs were counted in 0.5% intervals (Fig. S1).

To analyse introgression size and distribution, we used the same SNP matrix as for counting crossovers. Introgressions were detected as contiguous homozygous wild barley alleles or heterozygous positions along the chromosome. The mean distance between the first or last marker position of each contiguous region and the previous or next marker, respectively, defined the size of an introgression, and the mean of the first and last marker defined its central position. We calculated Spearman's rank correlation coefficient (ρ) between the size of an introgression (Mb) and the local recombination rate (LRR, cM Mb^{-1}) in a given 0.5% chromosomal interval to analyse the correlation between introgression size and LRR. Similarly, we calculated Spearman's rank correlation coefficient (ρ) between genome-wide mean introgression size (Mb) and GWRR (cM Mb^{-1}). GWRR was calculated by summarizing recombination frequencies between marker pairs along each chromosome (M, cM = M × 100) and dividing by a total genome size of 5300 Mb.

Genome-wide association analysis

Genome-wide association analysis was performed using the total number of crossovers accumulated over nine meiotic divisions as a quantitative phenotypic trait. SNPs which were monomorphic in a specific subpopulation were coded as 0 (i.e. domesticated 'Barke' allele). Missing SNPs (0.77% of all SNPs) were imputed using the mean score of polymorphic flanking markers (matrix E (Maurer & Pillen, 2019), https://doi.org/10.5447/ipk/2019/20).

The scan for genome-wide marker trait associations followed a robust three-step procedure performed in SAS 9.4 (SAS Institute Inc., Cary, NC, USA). (1) The whole set of SNPs was included in a multiple linear regression model to find potentially associated SNPs based on stepwise selection with SAS PROC GLMSELECT. For this, 80% of phenotype data were randomly assigned to the prediction set and 20% were assigned to the validation set. SNPs were consecutively included in the final model as long as they were able to decrease the average square error (ASE) of phenotype prediction in the validation set. This procedure was repeated 100 times with independent random assignments and the number of times an SNP was included in the final model was recorded. Only those SNPs that were included in more than one out of 100 models were treated as robust enough to be included in the second step. (2) A second model fitting was performed with the SNPs selected in step 1. This model included the whole phenotype dataset and stepwise selection of SNPs based on minimizing the Schwarz Bayesian Criterion (SBC (Schwarz, 1978)) with SAS PROC GLMSELECT. The list of selected SNPs, hereafter called cofactors, was then included in the third step. (3) Each single SNP was finally screened for significance by multiple linear regression with the cofactors modelled in the background with SAS PROC REG.

Additionally, we applied a second layer of cross-validation to remove the effects of local recombination rate modifiers (Jordan et al., 2018). Briefly, we screened only markers of a given chromosome for associations with the number of crossovers on the remaining chromosomes based on the procedure mentioned above. Using this approach, the effects of local recombination rate variation are reduced and trans-acting recombination rate modifiers are identified.

Exome capture data analysis

Exome capture reads first passed a quality enrichment process to remove sequence adapter remains and low-quality sequences using TRIMGALORE (https://github.com/FelixKrueger/TrimGalore). Subsequently, quality-improved reads were aligned with BWA MEM (Li, 2013) to the barley genome reference sequence (version 2) of cv Morex (Monat et al., 2019). From the constructed alignments read duplicates were removed by SAMTOOLS (Li et al., 2009). We then merged the 1420 HEB-25 lines across the 25 families into a single BAM file. This file was used for SNP calling using FREEBAYES (Garrison & Marth, 2012) applying parameter '--min-alternate-count 3 --min-alternate-fraction 0.05 --min-coverage 10 --no-complex --dont-left-align-indels --no-population-priors'. High-quality SNPs were filtered by BCFTOOLS

(Li, 2011) in which each SNP is required to have a vcf quality score above 1000. The respective REC8 gene (HORVU.MOREX.r2.1HG0075790) was extracted using BED-TOOLS 'intersect' (Quinlan & Hall, 2010). Constructed alignment files and the matrix of filtered SNPs (Data Citation DOI_1) from 1420 HEB-25 lines are available for the REC8 candidate gene in the PGP repository (Arend *et al.*, 2016). Respective DOIs were generated using E!DAL (Arend *et al.*, 2014).

Candidate gene analysis

Candidate gene analysis was performed by manually screening all annotated high-confidence genes in a ± 0.5 cM window surrounding the quantitative trait locus (QTL). Genetic map positions were derived from Maurer *et al.* (2015). Furthermore, orthologues of known meiotic genes described by Mercier *et al.* (2015) were identified using PLAZA (https://bioinformatics.psb.ugent.be/plaza/versions/plaza_v4_5_monocots/) (Vandepoele *et al.*, 2013; Van Bel *et al.*, 2018). The physical positions of putative orthologues of known meiotic genes were used to assist candidate gene analysis. A candidate gene located within the 0.5 cM window surrounding the QTL was tested for allelic variation within the entire population using SNPs identified by exome capture. SNPs within the candidate gene were then tested for their association with the crossover phenotype, assuming that the wild barley allele is dominant in the case of rare heterozygous genotypes. First, a one-way ANOVA was performed followed by Tukey's honest significant difference test to analyse the effects of each SNP. Gene models were retrieved from the EnsemblPlants database (Release 46) (Cunningham *et al.*, 2019). Gene expression data were retrieved from BARLEX (The Barley Genome Explorer; Colmsee *et al.*, 2015; Mascher *et al.*, 2017).

Results and discussion

Recombination rate variation in 25 intraspecific hybrid populations between wild and domesticated barley

To explore natural variation in meiotic recombination rates, we took advantage of the barley population HEB-25 derived from a cross between one domesticated barley cultivar ('Barke') and 25 wild barley accessions (Badr *et al.*, 2000; Maurer *et al.*, 2015). Each of the 25 subpopulations was propagated for eight generations ($BC_1S_{3:8}$) via self-pollination resulting in a total of nine meiotic divisions over the course of which recombination events were accumulated. A total of 1340 lines (21–72 lines per subpopulation) were subjected to high-resolution SNP genotyping on the barley 50k iSelect array, yielding a total of 32 120 physically mapped SNPs (Bayer *et al.*, 2017; Monat *et al.*, 2019). After removing subpopulation-specific monomorphic SNPs and SNPs with a minor allele frequency of <0.1, a total set of 7174–11 246 SNPs with a mean inter-SNP distance of 386–669 kb was used to measure meiotic recombination events.

We measured an average of 22.17 crossovers (range 18.7–25.6) across all subpopulations, indicating quantitative variation in

total crossover number almost resembling a normal distribution (Fig. 1b, Shapiro–Wilk normality test, $P = 0.043$). The average number of crossovers detected in population HEB-25 seemed lower than would be expected over nine meiotic divisions assuming an average of 10 crossovers per generation accumulated over nine meiotic divisions (Phillips *et al.*, 2015; Dreissig *et al.*, 2017). However, as heterozygosity decreased by 50% per generation in inbreeding barley (Morrell *et al.*, 2003; Abdel-Ghani *et al.*, 2004), so did our ability to detect crossovers.

Given the difference of 6.9 crossovers between the two subpopulations at the ends of the scale, we looked at each subpopulation's recombination landscape to understand the nature of this increase in crossover number (Tukey's HSD test, $P = 0.0068$, Fig. S3). Interestingly, comparing recombination rates (cM Mb^{-1}) between the two most extreme subpopulations 23 and 24 along each chromosome showed a tendency towards an increase across low-recombining pericentromeric regions as well as distal subtelomeric regions in subpopulation 23 (Fig. 2a,c). This difference was not explained by a higher number of SNPs in one population, nor did we observe a correlation between differences in SNP number and the number of crossovers measured across the entire population (Fig. 2e,f; Pearson's $r = -0.04$, $P = 0.08$). Our observation was confirmed by summarizing mean recombination rates (cM Mb^{-1}) across the low-recombining pericentromeric interval (25–75%) of all seven barley chromosomes, showing a difference of 0.13 cM Mb^{-1} (Welch's two-sample t-test, $P = 0.042$). Again, this increase in recombination rate did not stem from a difference in SNP number (Welch's two-sample t-test, $P = 0.513$, difference in mean SNP number = 0.3 across the 25–75% interval). No significant increase was observed in the 75–100% distal region ($+ 0.319$ cM Mb^{-1}, Welch's two-sample t-test, $P = 0.089$), and in the 0–25% region ($+ 0.27$ cM Mb^{-1}, $P = 0.28$).

Regarding the underlying causes, a multitude of genetic, epigenetic and structural factors influencing recombination rates have been described in various organisms. Allelic variation in pro-crossover factors, that is the ubiquitin E3 ligase *HEI10* (Ziolkowski *et al.*, 2017), or simultaneous mutation of anti-crossover factors *RECQ4a*, *RECQ4b* and combination with increased *HEI10* copy number (Serra *et al.*, 2018), was shown to result in a massive increase in recombination rate in distal chromosomal regions in Arabidopsis, but not across the pericentromere. Between closely related *Drosophila* species, allelic variation in a single gene (*MEI17*/*MEI18*) explained large differences in both the rate and the patterning of recombination events (Brand *et al.*, 2018). In plants, a shift in the patterning of recombination events was shown to be linked to DNA methylation in non-CG sequence contexts and histone 3 lysine 9 dimethylation (H3K9me) (Underwood *et al.*, 2018). A possibly confounding factor in population HEB-25 may be structural variations, as these were shown to affect crossover patterning at multiple scales, that is SNPs inhibiting crossovers at base-pair resolution, juxtapositioning of homozygous and heterozygous regions shifting crossovers into heterozygous regions, and inversions inhibiting crossovers at the megabase scale (Borts & Haber, 1987; Drouaud *et al.*, 2006; Ziolkowski *et al.*, 2015; Rowan *et al.*, 2019; Jiao &
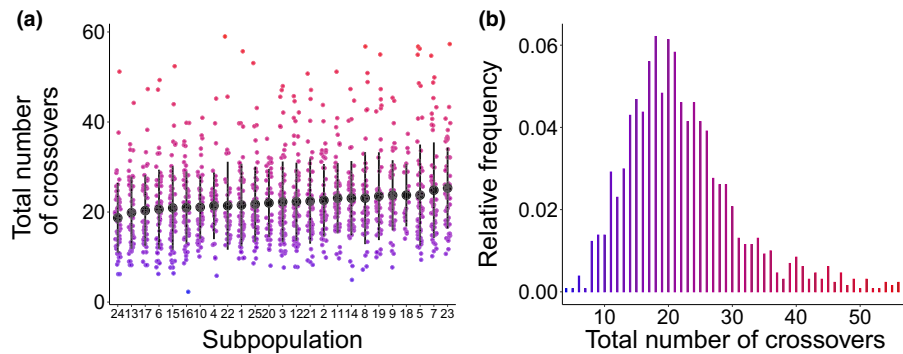
Fig. 1 Crossover variation in 25 subpopulations of the barley NAM population HEB-25. (a) Total number of crossovers accumulated over nine rounds of meiosis (*y*-axis) shown for each subpopulation (*x*-axis). Each dot represents an individual HEB line of a given subpopulation. Mean crossover number of each subpopulation is shown in black with error bars indicating the standard deviation of each subpopulation. (b) Frequency distribution of total crossover number across the entire population.
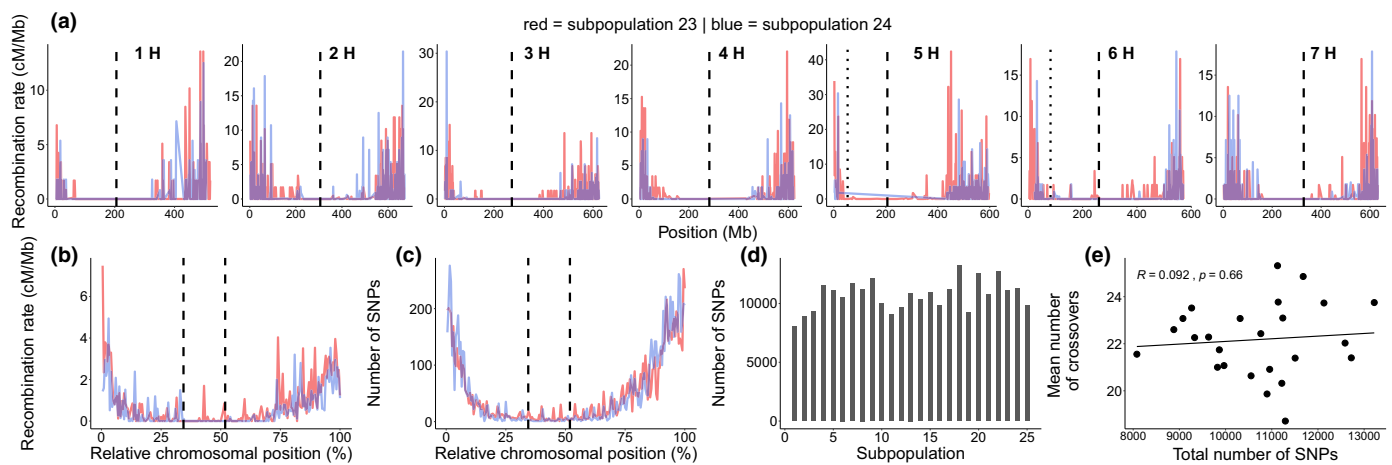
Fig. 2 Comparison of recombination landscapes between two extreme HEB-25 subpopulations. (a) Comparison of chromosomal recombination landscapes (1H to 7H) between high-recombining (red) and low-recombining (blue) subpopulations (subpopulation 23 vs 24, *Hordeum vulgare* L. × *Hordeum vulgare* subsp. *spontaneum* (K. Koch) Thell). (b) Genome-wide mean recombination rate of the high- and low-recombining subpopulations showing a genome-wide increase across pericentromeric regions. (c) Genome-wide mean SNP density of high- and low-recombining subpopulations. (d) Total number of unfiltered SNPs of each subpopulation. (e) Correlation between total crossover number and total number of unfiltered SNPs for each subpopulation (Pearson's $r = 0.092$, $P = 0.66$). Each dot represents one subpopulation. Centromere positions and nucleolus organizer regions (NORs) are shown as dashed lines and dotted lines, respectively.

Schneeberger, 2020). As our SNP array data did not allow us to identify structural variations such as inversions, we instead focused on the possibly confounding effects of SNP density and total number of SNPs. A higher number of SNPs may simply increase the probability of detecting crossovers. Between the two populations showing the highest and lowest number of crossovers, the total number of SNPs was almost identical (11 125 and 11 294, respectively). Across the entire population, we did not observe a correlation between differences in SNP number and crossovers (Pearson's $r = -0.04$, $P = 0.85$, Fig. 2f). There was, however, a strong correlation between SNP density and recombination frequency at the chromosome level (Fig. S4). This is in strong agreement with previous studies reporting positive correlations between SNP density, recombination frequency and gene density in other small- or large-genome plants (Mascher *et al.*, 2017; Darrier *et al.*, 2017; Jordan *et al.*, 2018; Kianian *et al.*, 2018; Gardiner *et al.*, 2019; Rowan *et al.*, 2019). Given the

suppressive effects of chromosomal inversions, their rather low frequency and small size (few Mb) previously shown in barley make them unlikely to contribute to genome-wide differences in recombination patterning (Konishi & Linde-Laursen, 1988; Keilwagen *et al.*, 2019). Another possibly confounding factor is the environment. Because population HEB-25 was propagated under field conditions, differences in flowering time may result in meiosis taking place at different temperatures, which would affect recombination rates (Phillips *et al.*, 2015; Lloyd *et al.*, 2018). To test this, we looked at the correlation between total crossover number and flowering time data reported by (Maurer *et al.*, 2015). The absence of a correlation between flowering time and crossover number indicated that differences in flowering time probably did not result in meiosis taking place at extremely different temperatures (Pearson's $r = -0.048$, $P = 0.084$, Fig. S5).

Although the effects of structural variations and environmental conditions could not be fully excluded in our population, we did

consider the presence of *trans*-acting recombination rate modifiers.

Identification of trans-acting recombination rate modifiers

To identify genetically determined recombination rate modifiers in our intraspecific hybrid population, we performed a genome-wide association study (GWAS). We utilized quantitative variation in the total number of crossovers per line and associated these with the genotype of each line. Using this approach, we were associating the number of crossovers accumulated over nine meiotic divisions with the genotypic constitution of the final generation ($BC_1S_{3:8}$), which did not allow us to determine whether a recombination rate modifier was present/absent or homozygous/heterozygous throughout previous meiotic divisions. Therefore, as already argued by others, we are systematically underestimating the effects of recombination rate modifiers and are only detecting dominant modifiers with strong effects (Esch *et al.*, 2007; Jordan *et al.*, 2018; Gardiner *et al.*, 2019). Furthermore, to identify *trans*-acting recombination rate modifiers rather than identifying common recombination breakpoints, we applied a cross-validation step in which SNPs of a given chromosome were only screened for associations with the number of crossovers on the remaining six chromosomes (Jordan *et al.*, 2018). Finally, only those QTLs retained after cross-validation were considered *trans*-acting recombination rate modifiers. Throughout both types of cross-validation (Maurer *et al.*, 2015; Jordan *et al.*, 2018) we consistently detected one significant QTL on chromosome 1H (Fig. 3, $-\log_{10} P = 9.1$, $-\log_{10}$ Bonferroni threshold $= 6.5$) with an effect size of the wild barley allele of $+42\%$ (i.e. $+7.84$ total crossovers, minor allele frequency of 0.03) that explained 3% of the total variation observed across the entire population (hereafter named 1H.recQTL1, Dataset S2).

By screening a total of 37 annotated high-confidence genes (Mascher *et al.*, 2017; Monat *et al.*, 2019) in a ± 0.5 cM (2 243 219 bp) window surrounding 1H.recQTL1, we identified the meiosis-specific kleisin cohesin subunit *REC8* as a candidate gene genetically linked within 0.3 cM and physically separated by 1.8 Mb (Dataset S3). *Hordeum vulgare REC8* (*HvREC8*) exists in two copies, HORVU.MOREX.r2.1HG0050790 and HORVU.MOREX.r2.1HG0075790, both located on chromosome 1H at 422 and 513 Mb, respectively. However, only the latter gene is closely linked to the significantly associated SNP within a distance of 1.8 Mb. Both *REC8* genes show expression peaks in developing inflorescences (1–1.5 cm) and high similarity to *REC8* orthologues in related *Triticeae* species (Figs S6, S7; Colmsee *et al.*, 2015; Beier *et al.*, 2017; Mascher *et al.*, 2017). An essential prerequisite for a putative candidate gene is to show allelic variation within the population. Otherwise, if all individuals harboured the same variant of the gene, it would be unlikely to be the cause of recombination rate variation. Therefore, we used exome capture data of the entire population to search for SNPs within the presumably causative *HvREC8* paralogue (i.e. HORVU.MOREX.r2.1HG0075790). We identified a total of five high-confidence SNPs located within two exons and two introns, which differentiate the *HvREC8* variant of the

domesticated cultivar from those of the 25 wild barley accessions (Fig. 3b,c). By looking at the effects of each SNP on total crossover number, we identified three out of five SNPs showing a significant effect on total crossover number (Fig. 3d, Tukey's HSD $P < 0.05$). Interestingly, both intron variants (SNP_2 and SNP_5) were associated with an increase in crossover number ($+11.8$ and $+6.8\%$, respectively) and occurred exclusively in different subpopulations (Fig. 3c). These intron variants may affect mRNA splicing and could be of regulatory function (Pagani & Baralle, 2004). In cattle, REC8 intron variants were also identified as *trans*-acting recombination rate modifiers, suggesting a regulatory mode of action potentially conserved across kingdoms (Sandor *et al.*, 2012). Both intron variants seem to be located in conserved intron regions in related Triticeae species (Fig. S7). By contrast, a synonymous SNP (SNP_3) located in exon 9 of *HvREC8* was associated with a reduction in crossover number (-24.3%) and occurred in subpopulation 15 only (Fig. 3c). This SNP is located in a region where the barley genomic sequence differs from those of related Triticeae species. Whether these SNPs have a causative role in recombination rate variation or whether other not yet identified polymorphisms play a role cannot be answered here and remains to be addressed in future studies. However, our data support the idea of different *HvREC8* variants being present in wild barley.

Regarding the function of *REC8*, it was recently shown that REC8 occupancy is enriched in gene bodies, exons, GC-rich sequences and H3K27me3-modified genes in Arabidopsis (Lambing *et al.*, 2020). REC8 is involved in tethering chromatin loops to the chromosome axis and its abundance is highest in pericentromeric regions and correlates with crossover suppression (Kugou *et al.*, 2009; Ito *et al.*, 2014; Sun *et al.*, 2015; Folco *et al.*, 2017; Patel *et al.*, 2019; Schalbetter *et al.*, 2019; Köhler *et al.*, 2020; Lambing *et al.*, 2020). *REC8* was also identified in sheep, cattle and red deer as a factor mediating quantitative differences in genome-wide recombination rates (Sandor *et al.*, 2012; Johnston *et al.*, 2016, 2018). Interestingly, Sandor *et al.* (2012) also identified *REC8* intron variants associated with recombination rate variation, suggesting alternative regulation of *REC8* alleles as the causative agent. A different variant of *REC8*, altered gene expression or protein structure may have an effect on chromatin loop structure and therefore result in a pericentromeric region that is more permissive for crossovers to occur, as is evident in population HEB-25.

Patterns of introgression are shaped by local and genome-wide recombination rate variation

In intra- or interspecific hybrids, the minor parent genome (i.e. the parental genome being introgressed) may introduce beneficial or deleterious alleles into the major parent genome (Brown *et al.*, 1989; Martin & Jiggins, 2017; Schumer *et al.*, 2018). Linkage drag (i.e. the simultaneous introgression of deleterious alleles along with beneficial alleles) is a result of alleles being genetically linked by low local recombination rates, a universal genetic phenomenon observed across kingdoms (Harris & Nielsen, 2016; Juric *et al.*, 2016). It is of great hindrance in plant breeding and
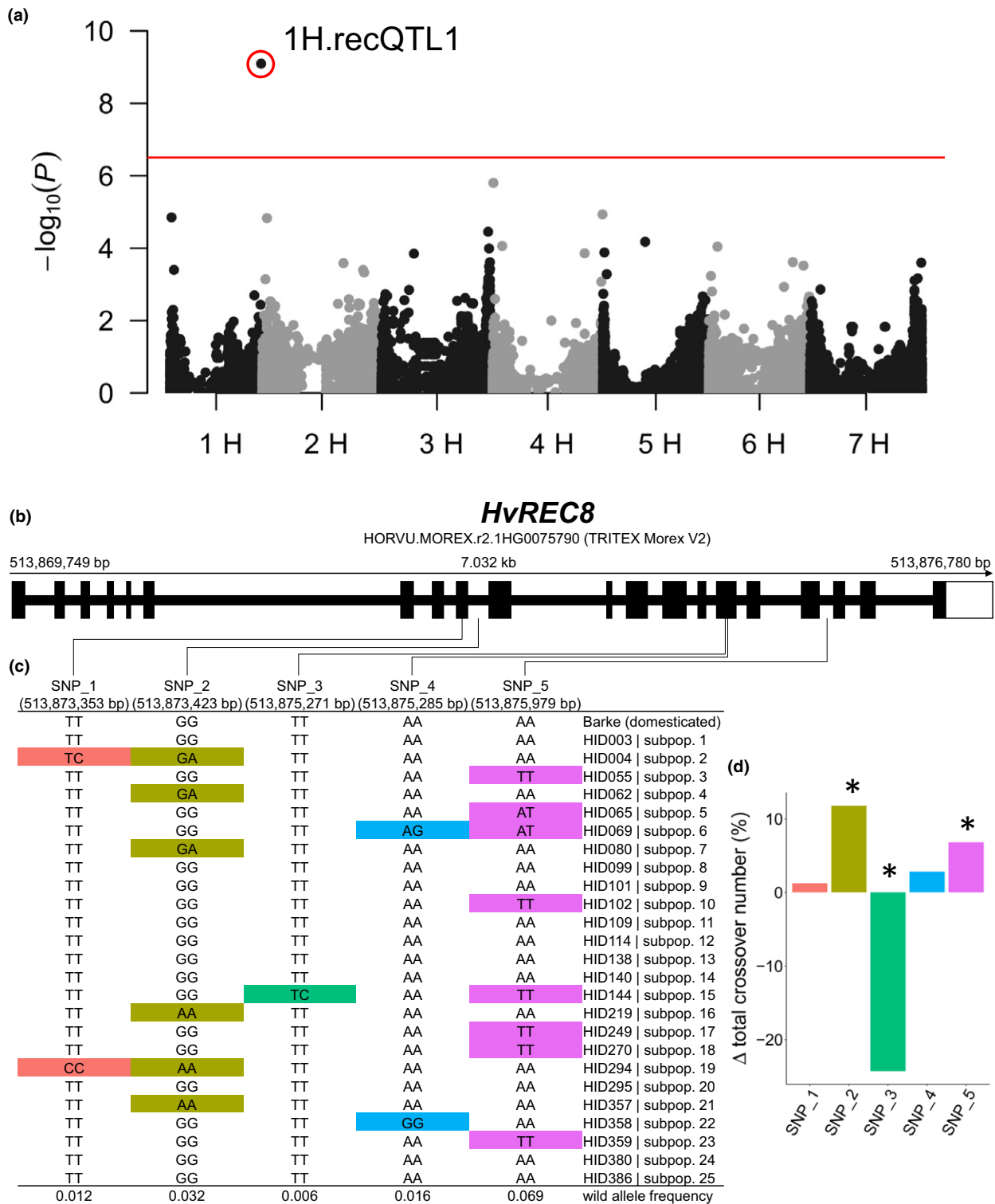
Fig. 3 Genome-wide association analysis for *trans*-acting recombination rate modifiers. (a) Manhattan-plot showing the *trans*-acting recombination rate QTL 1H.recQTL1 (black dot outlined in red) identified after cross-validation ($-\log_{10}P = 9.1$, effect size $= +42\%$ (i.e. $+7.8$ crossovers), $r^2 = 0.03$, minor allele frequency $= 0.03$). The Bonferroni threshold ($6.507 = -\log_{10}(0.01/32,120)$) is shown as a red line. (b) Exon and intron structure of *HvREC8* (HORVU.MOREX.r2.1HG0075790 (TRITEX Morex V2 assembly)). Exons are shown as large black rectangles. Introns are represented by a black line between exons. The 3′-untranslated region is shown as a white rectangle. (c) Positions and alleles of five SNPs within *HvREC8* identified among the 26 parents of the population. Alleles which deviate from the domesticated barley line are highlighted in colour. Allele frequencies of each SNP across the entire population are shown below. (d) Effects of five individual SNPs of *HvREC8* (HORVU.MOREX.r2.1HG0075790 (TRITEX Morex V2 assembly)) on total crossover number compared to the domesticated barley allele (difference in per cent). Asterisks indicate significant effects determined by ANOVA followed by Tukey's honest significant difference test ($P < 0.05$).

plays an important role in the evolution of hybrid genomes (Brown *et al.*, 1989; Schumer *et al.*, 2018; Martin *et al.*, 2019). However, there is little empirical data exploring the relationship between recombination rates and patterns of introgression in intraspecific hybrid populations.

Given the amount of local and genome-wide recombination rate variation we observed in population HEB-25, we investigated how the size and position of introgressions were shaped over relatively few generations. Wild barley (minor parent) introgressions into the domesticated parent (major parent) genome were detected as contiguous wild barley alleles along the chromosome. We detected a total of 19 635 wild barley introgressions of varying size, ranging from < 1 to 670 Mb (Fig. S8). By plotting the size of each introgression against its position on the chromosome, we observed a striking relationship between local recombination rate and introgression size (Figs 4, 5a,b; Spearman's rank correlation $\rho = -0.9$, $P < 2.2 \times 10^{-6}$).

As one would intuitively assume, introgressions were smaller in regions of high recombination and larger in regions of low recombination. Heterozygous introgressions were generally smaller than homozygous introgressions, demonstrating that meiotic recombination events were continuously shrinking heterozygous regions until fixed as homozygous regions. Along the chromosome, introgressions in distal high-recombining regions ranged from < 1 to 200 Mb in size, whereas most introgressions in pericentromeric low-recombining regions ranged from 400 to 600 Mb. This shows how patterns of introgression were directly shaped by local recombination rate in the absence of selection. As a consequence, naturally occurring introgressions between wild and domesticated species would exhibit varying deleterious burdens on the major parent genome depending on local recombination rate. In strictly self-fertilizing species, such as barley, introgressions are rapidly fixed in a homozygous state and thereby permanently fixed in size as well. This is directly relevant to mapping genes or QTLs via LD (LD-mapping), as large introgressions in low-recombining regions do not permit accurate mapping.

In addition to local recombination rate variation, we also observed genome-wide differences. A genome-wide increase in recombination rate in a given population would predict smaller introgressions and thereby reduced linkage drag and increase the efficiency of selection (Martin & Jiggins, 2017). We summarized the genome-wide recombination rate (cM Mb^{-1}) of each subpopulation and compared it to its average introgression size (Fig. 5c,d).

However, we did not detect strong correlations between genome-wide recombination rate and mean introgression size, and only heterozygous introgressions were significantly correlated with the genome-wide recombination rate (Spearman's rank correlation $\rho = -0.41$, $P = 0.042$). This probably reflects that local recombination rate variation along the chromosome is usually greater than genome-wide recombination rate variation between
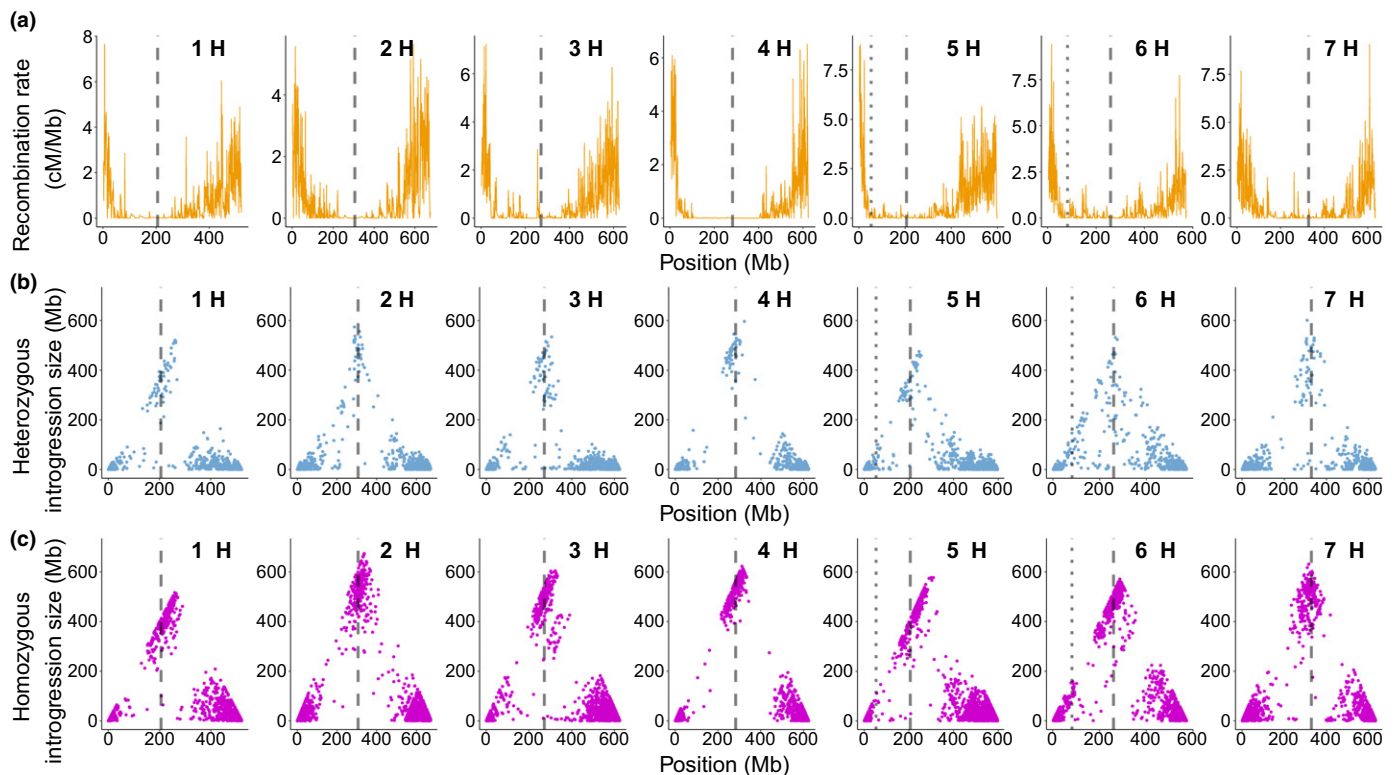
Fig. 4 Relationship between wild barley introgressions and recombination rates in intraspecific hybrid populations. (a) Mean recombination rate (cM Mb^{-1}, *y*-axis) of the entire population along the physical length of each chromosome (Mb, *x*-axis). (b, c) Size (Mb, *y*-axis) and position (Mb, *x*-axis) of heterozygous (b) and homozygous (c) wild barley introgressions for each chromosome. Each dot represents the centre of an introgression. Centromere positions and nucleolus organizer regions (NORs) are indicated by dashed and dotted lines, respectively.
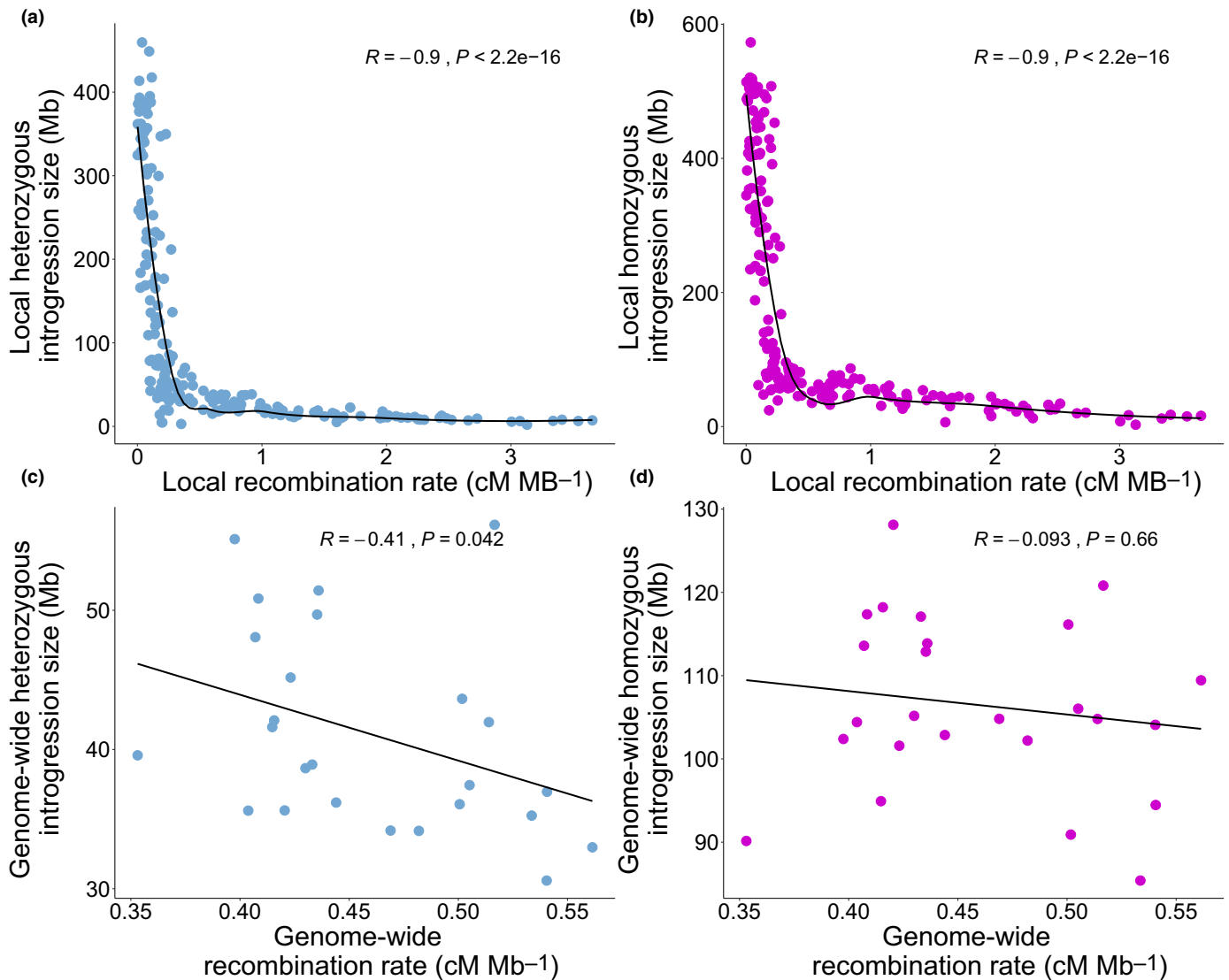
Fig. 5 Correlation between recombination rate and introgression size. (a, b) Correlation between size of heterozygous (a) or homozygous (b) wild barley introgressions (Mb, y-axis) and local recombination rate (cM Mb^{-1}, x-axis) determined in relative chromosomal intervals of 0.5%. (c, d) Correlation between genome-wide recombination rate (cM Mb^{-1}, x-axis) and genome-wide mean size (Mb, y-axis) of heterozygous (c) or homozygous (d) introgressions for each subpopulation.

subpopulations (i.e. 0–8 cM Mb^{-1} along the chromosome and 0.35–0.55 cM Mb^{-1} between subpopulations). As such, rather small differences in genome-wide recombination rate do not strongly explain differences in genome-wide mean introgression size.

Taken together, we conclude that the effects of local recombination rate variation on patterns of introgression are stronger than those exerted by genome-wide differences, at least in this experimental population. This is expected due to stronger recombination rate variation along the chromosome than between individuals or populations. However, as we did observe similar tendencies for the effects of local and genome-wide recombination rate variation on patterns of introgression, we have been able to provide empirical evidence for a genomic phenomenon that was previously largely supported by intuition, rather than experimental data.

Project DEAL. The authors declare that they have no competing interests.

Author contributions

SD analysed the data regarding recombination, candidate genes and introgression, and conceptualized and wrote the manuscript. AM analysed raw SNP data, performed the GWAS, and wrote and edited the manuscript. RS, LM and AJF collected the exome capture data and edited the manuscript. TS analysed the exome capture data, and wrote and edited the manuscript. KP coordinated the project and edited the manuscript. All authors read and approved the final manuscript.

ORCID

Steven Dreissig (iD) https://orcid.org/0000-0002-4766-9698
Andreas Maurer (iD) https://orcid.org/0000-0002-2916-7475
Klaus Pillen (iD) https://orcid.org/0000-0003-4646-6351
Thomas Schmutzer (iD) https://orcid.org/0000-0003-1073-6719

Data availability

Plant material is available from Klaus Pillen (klaus.pillen@landw.uni-halle.de) upon request. Genotype data have been deposited on e!DAL (https://doi.org/10.5447/ipk/2019/20). Crossover data are available in Dataset S1. Exome capture data of the *rec8* candidate gene have been deposited on e!DAL (preliminary link for Data Citation doi: https://doi.ipk-gatersleben.de/DOI/f388f054-8d33-4cc7-9d45-6cf6ee34a872/4db2694f-5962-4fd1-8661-eeaf0ed1d57d/2/1847940088). GWAS results are available in Dataset S2. Genes surrounding 1H.recQTL1 and relative expression values across 16 tissues are provided in Dataset S3.

References

Abdel-Ghani AH, Parzies HK, Omary A, Geiger HH. 2004. Estimating the outcrossing rate of barley landraces and wild barley populations collected from ecologically different regions of Jordan. *Theoretical and Applied Genetics.* **109**: 588–595.

Arend D, Junker A, Scholz U, Schüler D, Wylie J, Lange M. 2016. PGP repository: a plant phenomics and genomics data publication infrastructure. *Database* **2016**: baw033.

Arend D, Lange M, Chen J, Colmsee C, Flemming S, Hecht D, Scholz U. 2014. e!DAL – a framework to store, share and publish research data. *BMC Bioinformatics* **15**: 214.

Arnold BJ, Lahner B, DaCosta JM, Weisman CM, Hollister JD, Salt DE, Bomblies K, Yant L. 2016. Borrowed alleles and convergence in serpentine adaptation. *Proceedings of the National Academy of Sciences, USA* **113**: 8320–8325.

Badr A, Müller K, Schäfer-Pregl R, El Rabey H, Effgen S, Ibrahim HH, Pozzi C, Rohde W, Salamini F. 2000. On the origin and domestication history of barley (*Hordeum vulgare*). *Molecular Biology and Evolution* **17**: 499–510.

Bayer MM, Rapazote-Flores P, Ganal M, Hedley PE, Macaulay M, Plieske J, Ramsay L, Russell J, Shaw PD, Thomas W *et al*. 2017. Development and evaluation of a barley 50k iSelect SNP array. *Frontiers in Plant Science* **8**: 1792.

Beier S, Himmelbach A, Colmsee C, Zhang X-Q, Barrero RA, Zhang Q, Li L, Bayer M, Bolser D, Taudien S *et al*. 2017. Construction of a map-based reference genome sequence for barley, *Hordeum vulgare* L. *Scientific Data* **4**: 170044.

Blackmon H, Adams RH, Anya. 2015. *EvobiR: Tools for comparative analyses and teaching evolutionary biology, v.1.1.* Zenodo. [WWW document] doi: 10.5281/zenodo.30938.

Börner GV, Kleckner N, Hunter N. 2004. Crossover/noncrossover differentiation, synaptonemal complex formation, and regulatory surveillance at the leptotene/zygotene transition of meiosis. *Cell* **117**: 29–45.

Borts RH, Haber JE. 1987. Meiotic recombination in yeast: alteration by multiple heterozygosities. *Science* **237**: 1459–1465.

Brand CL, Cattani MV, Kingan SB, Landeen EL, Presgraves DC. 2018. Molecular evolution at a meiosis gene mediates species differences in the rate and patterning of recombination. *Current Biology* **28**: 1289–1295.

Brown AHD, Lawrence GJ, Jenkin M, Douglass J, Gregory E. 1989. Linkage drag in backcross breeding in barley. *Journal of Heredity* **80**: 234–239.

Choi K, Zhao X, Kelly KA, Venn O, Higgins JD, Yelina NE, Hardcastle TJ, Ziolkowski PA, Copenhaver GP, Franklin FCH *et al*. 2013. Arabidopsis meiotic crossover hot spots overlap with H2A.Z nucleosomes at gene promoters. *Nature Genetics* **45**: 1327–1336.

Choi K, Zhao X, Tock AJ, Lambing C, Underwood CJ, Hardcastle TJ, Serra H, Kim J, Cho HS, Kim J *et al*. 2018. Nucleosomes and DNA methylation shape meiotic DSB frequency in *Arabidopsis thaliana* transposons and gene regulatory regions. *Genome Research.* **28**: 532–546.

Colmsee C, Beier S, Himmelbach A, Schmutzer T, Stein N, Scholz U, Mascher M. 2015. BARLEX – the barley draft genome explorer. *Molecular Plant* **8**: 964–966.

Corpet F. 1988. Multiple sequence alignment with hierarchical clustering. *Nucleic Acids Research* **16**: 10881–10890.

Crown KN, Miller DE, Sekelsky J, Hawley RS. 2018. Local inversion heterozygosity alters recombination throughout the genome. *Current Biology* **28**: 2984–2990.

Cunningham F, Achuthan P, Akanni W, Allen J, Amode MR, Armean IM, Bennett R, Bhai J, Billis K, Boddu S *et al*. 2019. Ensembl 2019. *Nucleic Acids Research* **47**: D745–D751.

Darrier B, Rimbert H, Balfourier F, Pingault L, Josselin A-A, Servin B, Navarro J, Choulet F, Paux E, Sourdille P. 2017. High-resolution mapping of crossover events in the hexaploid wheat genome suggests a universal recombination mechanism. *Genetics* **206**: 1373–1388.

Dreissig S, Fuchs J, Himmelbach A, Mascher M, Houben A. 2017. Sequencing of single pollen nuclei reveals meiotic recombination events at megabase resolution and circumvents segregation distortion caused by postmeiotic processes. *Frontiers in Plant Science.* **8**: 1620.

Dreissig S, Mascher M, Heckmann S. 2019. Variation in recombination rate is shaped by domestication and environmental conditions in barley. *Molecular Biology and Evolution.* **36**: 2029–2039.

Drouaud J, Camilleri C, Bourguignon P-Y, Canaguier A, Bérard A, Vezon D, Giancola S, Brunel D, Colot V, Prum B *et al*. 2006. Variation in crossing-over rates across chromosome 4 of *Arabidopsis thaliana* reveals the presence of meiotic recombination 'hot spots'. *Genome Research* **16**: 106–114.

Esch E, Szymaniak JM, Yates H, Pawlowski WP, Buckler ES. 2007. Using crossover breakpoints in recombinant inbred lines to identify quantitative trait loci controlling the global recombination frequency. *Genetics* **177**: 1851–1858.

Fernandes JB, Wlodzimierz P, Henderson IR. 2019. Meiotic recombination within plant centromeres. *Current Opinion in Plant Biology* **48**: 26–35.

Folco HD, Chalamcharla VR, Sugiyama T, Thillainadesan G, Zofall M, Balachandran V, Dhakshnamoorthy J, Mizuguchi T, Grewal SIS. 2017. Untimely expression of gametogenic genes in vegetative cells causes uniparental disomy. *Nature* **543**: 126–130.

Gardiner L-J, Wingen LU, Bailey P, Joynson R, Brabbs T, Wright J, Higgins JD, Hall N, Griffiths S, Clavijo BJ *et al*. 2019. Analysis of the recombination landscape of hexaploid bread wheat reveals genes controlling recombination and gene conversion frequency. *Genome Biology* **20**: 69.

Garrison E, Marth G. 2012. Haplotype-based variant detection from short-read sequencing. *arXiv [q-bio.GN]*: https://arxiv.org/abs/1207.3907.

Haenel Q, Laurentino TG, Roesti M, Berner D. 2018. Meta-analysis of chromosome-scale crossover rate variation in eukaryotes and its significance to evolutionary genomics. *Molecular Ecology* **27**: 2477–2497.

New
Phytologist

Harris K, Nielsen R. 2016. The genetic cost of Neanderthal introgression. *Genetics* 203: 881–891.

He F, Pasam R, Shi F, Kant S, Keeble-Gagnere G, Kay P, Forrest K, Fritz A, Hucl P, Wiebe K *et al.* 2019. Exome sequencing highlights the role of wild-relative introgression in shaping the adaptive landscape of the wheat genome. *Nature Genetics* 51: 896–904.

Heliconius Genome Consortium. 2012. Butterfly genome reveals promiscuous exchange of mimicry adaptations among species. *Nature* 487: 94–98.

Higgins JD, Perry RM, Barakate A, Ramsay L, Waugh R, Halpin C, Armstrong SJ, Franklin FCH. 2012. Spatiotemporal asymmetry of the meiotic program underlies the predominantly distal distribution of meiotic crossovers in barley. *Plant Cell* 24: 4096–4109.

Huerta-Sánchez E, Jin X, Bianba Z, Peter BM, Vinckenbosch N, Liang Y, Yi X, He M, Somel M *et al.* 2014. Altitude adaptation in Tibetans caused by introgression of Denisovan-like DNA. *Nature* 512: 194–197.

Hufford MB, Xu X, van Heerwaarden J, Pyhäjärvi T, Chia J-M, Cartwright RA, Elshire RJ, Glaubitz JC, Guill KE, Kaeppler SM *et al.* 2012. Comparative population genomics of maize domestication and improvement. *Nature Genetics* 44: 808–811.

Ito M, Kugou K, Fawcett JA, Mura S, Ikeda S, Innan H, Ohta K. 2014. Meiotic recombination cold spots in chromosomal cohesion sites. *Genes to Cells* 19: 359–373.

Jiao W-B, Schneeberger K. 2020. Chromosome-level assemblies of multiple Arabidopsis genomes reveal hotspots of rearrangements with altered evolutionary dynamics. *Nature Communications* 11: 989.

Johnston SE, Bérénos C, Slate J, Pemberton JM. 2016. Conserved genetic architecture underlying individual recombination rate variation in a wild population of soay sheep (*Ovis aries*). *Genetics* 203: 583–598.

Johnston SE, Huisman J, Pemberton JM. 2018. A genomic region containing REC8 and RNF212B is associated with individual recombination rate variation in a wild population of red deer (*Cervus elaphus*). *G3* 8: 2265–2276.

Jordan KW, Wang S, He F, Chao S, Lun Y, Paux E, Sourdille P, Sherman J, Akhunova A, Blake NK *et al.* 2018. The genetic architecture of genome-wide recombination rate variation in allopolyploid wheat revealed by nested association mapping. *The Plant Journal* 95: 1039–1054.

Juric I, Aeschbacher S, Coop G. 2016. The strength of selection against Neanderthal introgression. *PLoS Genetics* 12: e1006340.

Keilwagen J, Lehnert H, Berner T, Beier S, Scholz U, Himmelbach A, Stein N, Badaeva ED, Lang D, Kilian B *et al.* 2019. Detecting large chromosomal modifications using short read data from genotyping-by-sequencing. *Frontiers in Plant Science* 10: 1133.

Kianian PMA, Wang M, Simons K, Ghavami F, He Y, Dukowic-Schulze S, Sundararajan A, Sun Q, Pillardy J, Mudge J *et al.* 2018. High-resolution crossover mapping reveals similarities and differences of male and female recombination in maize. *Nature Communications* 9: 2370.

Köhler S, Wojcik M, Xu K, Dernburg A. 2020. The interaction of crossover formation and the dynamic architecture of the synaptonemal complex during meiosis. *BioRxiv*. doi: 10.1101/2020.02.16.947804.

Konishi T, Linde-Laursen I. 1988. Spontaneous chromosomal rearrangements in cultivated and wild barleys. *Theoretical and Applied Genetics* 75: 237–243.

Kugou K, Fukuda T, Yamada S, Ito M, Sasanuma H, Mori S, Katou Y, Itoh T, Matsumoto K, Shibata T *et al.* 2009. Rec8 guides canonical Spo11 distribution along yeast meiotic chromosomes. *Molecular Biology of the Cell* 20: 3064–3076.

Künzel G, Korzun L, Meister A. 2000. Cytologically integrated physical restriction fragment length polymorphism maps for the barley genome based on translocation breakpoints. *Genetics* 154: 397–412.

Lam I, Keeney S. 2014. Mechanism and regulation of meiotic recombination initiation. *Cold Spring Harbor Perspectives in Biology* 7: a016634.

Lambing C, Tock AJ, Topp SD, Choi K, Kuo PC, Zhao X, Osman K, Higgins JD, Franklin FCH, Henderson IR. 2020. Interacting genomic landscapes of REC8-cohesin, chromatin, and meiotic recombination in Arabidopsis. *Plant Cell* 32: 1218–1239.

Lamichhaney S, Berglund J, Almén MS, Maqbool K, Grabherr M, Martinez-Barrio A, Promerová M, Rubin C-J, Wang C, Zamani N *et al.* 2015. Evolution of Darwin's finches and their beaks revealed by genome sequencing. *Nature* 518: 371–375.

Li H, Handsaker B, Wysoker A, Fennell T, Ruan J, Homer N, Marth G, Abecasis G, Durbin R; 1000 Genome Project Data Processing Subgroup. 2009. The sequence alignment/map format and SAMtools. *Bioinformatics* 25: 2078–2079.

Li H. 2011. A statistical framework for SNP calling, mutation discovery, association mapping and population genetical parameter estimation from sequencing data. *Bioinformatics* 27: 2987–2993.

Li H. 2013. Aligning sequence reads, clone sequences and assembly contigs with BWA-MEM. *arXiv [q-bio.GN]*. https://arxiv.org/abs/1303.3997.

Lloyd A, Morgan C, Franklin FC, Bomblies K. 2018. Plasticity of meiotic recombination rates in response to temperature in Arabidopsis. *Genetics* 208: 1409–1420.

Mallet J, Besansky N, Hahn MW. 2016. How reticulated are species? *BioEssays: News and Reviews in Molecular, Cellular and Developmental Biology* 38: 140–149.

Martin SH, Davey JW, Salazar C, Jiggins CD. 2019. Recombination rate variation shapes barriers to introgression across butterfly genomes. *PLoS Biology* 17: e2006288.

Martin SH, Jiggins CD. 2017. Interpreting the genomic landscape of introgression. *Current Opinion in Genetics & Development* 47: 69–74.

Mascher M, Gundlach H, Himmelbach A, Beier S, Twardziok SO, Wicker T, Radchuk V, Dockter C, Hedley PE, Russell J *et al.* 2017. A chromosome conformation capture ordered sequence of the barley genome. *Nature* 544: 427–433.

Maurer A, Draba V, Jiang Y, Schnaithmann F, Sharma R, Schumann E, Kilian B, Reif JC, Pillen K. 2015. Modelling the genetic architecture of flowering time control in barley through nested association mapping. *BMC Genomics* 16: 290.

Maurer A, Pillen K. 2019. 50k Illumina Infinium iSelect SNP Array data for the wild barley NAM population HEB-25. *e!DAL*. doi: 10.5447/ipk/2019/20.

Melamed-Bessudo C, Levy AA. 2012. Deficiency in DNA methylation increases meiotic crossover rates in euchromatic but not in heterochromatic regions in Arabidopsis. *Proceedings of the National Academy of Sciences, USA* 109: E981–E988.

Mercier R, Mézard C, Jenczewski E, Macaisne N, Grelon M. 2015. The molecular biology of meiosis in plants. *Annual Review of Plant Biology* 66: 297–327.

Mirouze M, Lieberman-Lazarovich M, Aversano R, Bucher E, Nicolet J, Reinders J, Paszkowski J. 2012. Loss of DNA methylation affects the recombination landscape in Arabidopsis. *Proceedings of the National Academy of Sciences, USA* 109: 5880–5885.

Monat C, Padmarasu S, Lux T, Wicker T, Gundlach H, Himmelbach A, Ens J, Li C, Muehlbauer GJ, Schulman AH *et al.* 2019. TRITEX: chromosome-scale sequence assembly of Triticeae genomes with open-source tools. *Genome Biology* 20: 284.

Morrell PL, Lundy KE, Clegg MT. 2003. Distinct geographic patterns of genetic diversity are maintained in wild barley (*Hordeum vulgare* ssp. *spontaneum*) despite migration. *Proceedings of the National Academy of Sciences, USA* 100: 10812–10817.

Pagani F, Baralle FE. 2004. Genomic variants in exons and introns: identifying the splicing spoilers. *Nature Reviews. Genetics* 5: 389–396.

Page SL, Hawley RS. 2003. Chromosome choreography: the meiotic ballet. *Science* 301: 785–789.

Patel L, Kang R, Rosenberg SC, Qiu Y, Raviram R, Chee S, Hu R, Ren B, Cole F, Corbett KD. 2019. Dynamic reorganization of the genome shapes the recombination landscape in meiotic prophase. *Nature Structural & Molecular Biology* 26: 164–174.

Phillips D, Jenkins G, Macaulay M, Nibau C, Wnetrzak J, Fallding D, Colas I, Oakey H, Waugh R, Ramsay L. 2015. The effect of temperature on the male and female recombination landscape of barley. *New Phytologist* 208: 421–429.

Quinlan AR, Hall IM. 2010. BEDTools: a flexible suite of utilities for comparing genomic features. *Bioinformatics* 26: 841–842.

Rowan BA, Heavens D, Feuerborn TR, Tock AJ, Henderson IR, Weigel D. 2019. An ultra high-density *Arabidopsis thaliana* crossover map that refines the influences of structural variation and epigenetic features. *Genetics* 213: 771–787.

Samuk K, Manzano-Winkler B, Ritz KR, Noor MAF. 2019. Natural selection shapes variation in genome-wide recombination rate in *Drosophila pseudoobscura*. *Current Biology*. **30**: 1517–1528.

Sandor C, Li W, Coppieters W, Druet T, Charlier C, Georges M. 2012. Genetic variants in *REC8*, *RNF212*, and *PRDM9* influence male recombination in cattle. *PLoS Genetics* **8**: e1002854.

Schalbetter SA, Fudenberg G, Baxter J, Pollard KS, Neale MJ. 2019. Principles of meiotic chromosome assembly revealed in *S. cerevisiae*. *Nature Communications* **10**: 4795.

Schumer M, Xu C, Powell DL, Durvasula A, Skov L, Holland C, Blazier JC, Sankararaman S, Andolfatto P, Rosenthal GG *et al.* 2018. Natural selection interacts with recombination to shape the evolution of hybrid genomes. *Science* **360**: 656–660.

Schwarz G. 1978. Estimating the dimension of a model. *Annals of Statistics* **6**: 461–464.

Schwarzkopf EJ, Motamayor JC, Cornejo OE. 2020. Genetic differentiation and intrinsic genomic features explain variation in recombination hotspots among cocoa tree populations. *BMC Genomics*. **21**: 332.

Serra H, Lambing C, Griffin CH, Topp SD, Nageswaran DC, Underwood CJ, Ziolkowski PA, Séguéla-Arnaud M, Fernandes JB, Mercier R *et al.* 2018. Massive crossover elevation via combination of *HEI10* and *recq4a recq4b* during Arabidopsis meiosis. *Proceedings of the National Academy of Sciences, USA* **115**: 2437–2442.

Sims J, Copenhaver GP, Schlögelhofer P. 2019. Meiotic DNA repair in the nucleolus employs a nonhomologous end-joining mechanism. *The Plant Cell* **31**: 2259–2275.

Stapley J, Feulner PGD, Johnston SE, Santure AW, Smadja CM. 2017. Variation in recombination frequency and distribution across eukaryotes: patterns and processes. *Philosophical Transactions of the Royal Society of London. Series B, Biological Sciences* **372**: 20160455.

Sun X, Huang L, Markowitz TE, Blitzblau HG, Chen D, Klein F, Hochwagen A. 2015. Transcription dynamically patterns the meiotic chromosome-axis interface. *eLife* **4**: e07424.

Tourrette E, Bernardo R, Falque M, Martin OC. 2019. Assessing by modeling the consequences of increased recombination in recurrent selection of *Oryza sativa* and *Brassica rapa*. *G3* **9**:4169–4181.

Underwood CJ, Choi K, Lambing C, Zhao X, Serra H, Borges F, Simorowski J, Ernst E, Jacob Y, Henderson IR *et al.* 2018. Epigenetic activation of meiotic recombination near *Arabidopsis thaliana* centromeres via loss of H3K9me2 and non-CG DNA methylation. *Genome Research* **28**: 519–531.

Van Bel M, Diels T, Vancaester E, Kreft L, Botzki A, Van de Peer Y, Coppens F, Vandepoele K. 2018. PLAZA 4.0: an integrative resource for functional, evolutionary and comparative plant genomics. *Nucleic Acids Research* **46**: D1190–D1196.

Vandepoele K, Van Bel M, Richard G, Van Landeghem S, Verhelst B, Moreau H, Van de Peer Y, Grimsley N, Piganeau G. 2013. pico-PLAZA, a genome database of microbial photosynthetic eukaryotes. *Environmental Microbiology* **15**: 2147–2153.

Wang J, Fan HC, Behr B, Quake SR. 2012. Genome-wide single-cell analysis of recombination activity and de novo mutation rates in human sperm. *Cell* **150**: 402–412.

Wendler N, Mascher M, Nöh C, Himmelbach A, Scholz U, Ruge-Wehling B, Stein N. 2014. Unlocking the secondary gene-pool of barley with next-generation sequencing. *Plant Biotechnology Journal* **12**: 1122–1131.

Yelina NE, Choi K, Chelysheva L, Macaulay M, de Snoo B, Wijnker E, Miller N, Drouaud J, Grelon M, Copenhaver GP *et al.* 2012. Epigenetic remodeling of meiotic crossover frequency in *Arabidopsis thaliana* DNA methyltransferase mutants. *PLoS Genetics* **8**: e1002844.

Yelina N, Diaz P, Lambing C, Henderson IR. 2015. Epigenetic control of meiotic recombination in plants. *Science China Life Sciences* **58**: 223–231.

Young ND, Tanksley SD. 1989. RFLP analysis of the size of chromosomal segments retained around the Tm-2 locus of tomato during backcross breeding. *Theoretical and Applied Genetics* **77**: 353–359.

Zelkowski M, Olson MA, Wang M, Pawlowski WP. 2019. Diversity and determinants of meiotic recombination landscapes. *Trends in Genetics* **35**: 359–370.

Zhang L, Liang Z, Hutchinson J, Kleckner N. 2014. Crossover patterning by the beam-film model: analysis and implications. *PLoS Genetics* **10**: e1004042.

Zickler D, Kleckner N. 1999. Meiotic chromosomes: integrating structure and function. *Annual Review of Genetics* **33**: 603–754.

Ziolkowski PA, Berchowitz LE, Lambing C, Yelina NE, Zhao X, Kelly KA, Choi K, Ziolkowska L, June V, Sanchez-Moran E *et al.* 2015. Juxtaposition of heterozygous and homozygous regions causes reciprocal crossover remodelling via interference during Arabidopsis meiosis. *eLife* **4**: e03708.

Ziolkowski PA, Underwood CJ, Lambing C, Martinez-Garcia M, Lawrence EJ, Ziolkowska L, Griffin C, Choi K, Franklin FCH, Martienssen RA *et al.* 2017. Natural variation and dosage of the HEI10 meiotic E3 ligase control Arabidopsis crossover recombination. *Genes & Development* **31**: 306–317.

Supporting Information

Additional Supporting Information may be found online in the Supporting Information section at the end of the article.

Dataset S1 Crossover counts across population HEB-25.

Dataset S2 Summary of GWAS for recombination rate modifiers

Dataset S3 List of genes surrounding 1H.recQTL1 and respective transcription profiles across 16 tissues

Fig. S1 SNP densities across all 25 subpopulations of HEB-25.

Fig. S2 Comparison of total crossover counts before and after removing outliers.

Fig. S3 Recombination landscapes of all 25 subpopulations of HEB-25.

Fig. S4 Genome-wide recombination frequency and SNP density of the entire population HEB-25.

Fig. S5 Correlation between crossover number and flowering time in population HEB-25.

Fig. S6 *HvREC8* transcription profile.

Fig. S7 *REC8* genomic sequence alignment across related monocotyledonous plants.

Fig. S8 Wild barley introgression size frequency distribution in population HEB-25.

Please note: Wiley Blackwell are not responsible for the content or functionality of any Supporting Information supplied by the authors. Any queries (other than missing material) should be directed to the *New Phytologist* Central Office.